International Journal of Pharmaceutics 386 (2010) 71–76

Contents lists available at ScienceDirect

International Journal of Pharmaceutics

journal homepage: www.elsevier.com/locate/ijpharm

Effect of drug chirality on the skin permeability of ibuprofen

F. Cilurzo*, E. Alberti, P. Minghetti, C.G.M. Gennari, A. Casiraghi, L. Montanari

Department of Pharmaceutical Sciences "Pietro Pratesi", Università degli Studi di Milano, via G. Colombo, 71 - 20133 (I) Milan, Italy

ARTICLE INFO

Article history:
Received 28 July 2009
Received in revised form 29 October 2009
Accepted 29 October 2009
Available online 10 November 2009

Keywords:
S-Ibuprofen
Supersaturation
Human skin permeability
Medicated plaster
Chirality

ABSTRACT

The *in vitro* passive diffusion of *S*-ibuprofen (*S*-IB) and *RS*-ibuprofen (*RS*-IB) through human epidermis was determined to study the effects of drug chirality. *S*-IB has a lower melting point (T_m = 54 °C) than *RS*-IB (T_m = 77 °C) and, therefore, a greater solubility (*S*-IB: 127 ± 1 μg/mL; *RS*-IB: 81 ± 1 μg/mL). Supersaturated plasters were prepared by using a poly(dimethylsiloxane) adhesive and Eugragit® RL and propylene glycol as antinucleant agents. The *in vitro* skin permeation profiles were determined by Franz cells and human epidermis obtained from three different donors. The permeation profiles of *S*-IB from saturated solutions resulted statistically higher than those of *RS*-IB ($p < 0.002$). When plasters were used, no differences were noticeable between the enantiomer and racemate ($p > 0.17$). The latter unexpected results could be explained considering that the *RS*-IB or *S*-IB *in vitro* release rate constants, determined using 3% w/w or 6% w/w loaded plasters, were not statistically different, suggesting that the drug diffusivity within the adhesive matrix represented the rate limiting step to the skin absorption.

1. Introduction

Ibuprofen (IB) is a chiral non-steroidal anti-inflammatory drug widely used in the treatment of musculoskeletal injuries. Even if the pharmacological activity of this drug resides in the *S*-enantiomer, IB is usually administrated as racemate (*RS*-IB) since an extensive bioconversion of the *R*-enantiomer to *S*-enantiomer occurs after oral administration (Cheng et al., 1994). The topical administration of IB allows patients to have a faster pain relief in comparison to the oral route followed by low plasma concentrations and thus low incidence of systemic side effects (Tegeder et al., 1999). Nevertheless, the skin metabolism does not result in the chiral inversion of (*R*)- to (*S*)-ibuprofen (*S*-IB) (Millership and Collier, 1997) and therefore, the anti-inflammatory effect is due to an half of the administered dose. The selection of *RS*-IB or *S*-IB is not only related to the drug intrinsic pharmacological activity, but also its physico-chemical properties. Indeed, the lower the melting point of the stereoisomer of a chiral compound, the higher the solubility in the vehicle and, consequently, the greater the flux through the skin (Touitou et al., 1994). The melting point of *S*-IB is about one third lower than the racemate and, thus, it is expected that its flux through human skin is higher than that of the racemate. Nevertheless, to the best of our knowledge, the skin permeability through human skin of *S*-IB and *RS*-IB has been not compared.

Moreover the design of the dosage form plays an important role in topical drug delivery as the composition of the vehicle influences the partitioning and/or the diffusivity of a drug and hence the absolute delivered amount. As far as *RS*-IB is concerned, supersaturated solutions (Iervolino et al., 2001) as well as supersaturated medicated plasters were effective to promote the drug skin permeation (Cilurzo et al., 2005). Such a plaster was developed by adding to a type of poly(dimethylsiloxane) pressure sensitive adhesive (PSA) propylene glycol and a poly(aminomethacrylate), namely Eudragit® RL100, which resulted effective as anti-nucleation agents and, therefore, able to promote the physical stability of the supersaturated adhesive matrix.

In the present work, the *in vitro* passive diffusion of *S*-IB and *RS*-IB through human epidermis was studied to evaluate the impact of drug chirality and vehicle on the permeation process. With this aim, *S*-IB and *RS*-IB saturated solutions and supersaturated plasters, prepared by using the same formulation proposed in a previous work (Cilurzo et al., 2005), were used as vehicles. Furthermore, since the drug loading and drug/excipients ratio can play a key role in the thermodynamic activity of the drug in the adhesive matrix and therefore influence the permeation through the skin, a formulative study was also carried out.

2. Materials and methods

2.1. Materials

S-Ibuprofen, *S*-IB (Francis, I); *RS*-ibuprofen, *RS*-IB; and propylene glycol, PG (ACEF, I); Eudragit® RL100, EuRL (Rofarma, I); BIO-PSA® 7-4602 (B46), the polymer content in ethyl acetate was 60% w/w (Dow Corning, USA). Backing layer: Cotran® 9715 membrane

* Corresponding author. Tel.: +39 02 50314635; fax: +39 02 50314657.
E-mail address: francesco.cilurzo@unimi.it (F. Cilurzo).

0378-5173/$ – see front matter © 2009 Elsevier B.V. All rights reserved.
doi:10.1016/j.ijpharm.2009.10.053

(3M, USA). Release liner: Scotchpak® 1022 film (3M, USA). Brufen crema® 10% m/m (Abbot SpA, I).

All solvents unless specified were of analytical grade.

2.2. Solubility determination

The solubility of *S*-IB and *RS*-IB was determined in deionized water at 32 ± 1 °C. The samples were stirred for 72 h to obtain saturated solutions. The solute in excess was removed by filtration. The saturated solutions were opportunely diluted in water and then analyzed by the HPLC method described in Section 2.8. The results are expressed as mean ± standard deviation of three replicates.

2.3. Thermal analysis

DSC data were recorded by using a DSC 2010 TA (TA Instruments, USA). The samples were sealed in aluminum pans and heated in inert atmosphere (70 mL/min N_2). The reference was an empty pan. The equipment was calibrated with an indium sample. Samples of *S*-IB or *RS*-IB were scanned at 10 K/min from 30 to 120 °C under nitrogen purging (70 mL/min).

2.4. Plaster preparation

The plasters were prepared by a casting and evaporation method. The mixtures were prepared in order to obtain dried plaster matrices with the composition reported in Table 1. Briefly, EuRL was preliminarily dissolved in ethyl acetate to get a 20% w/w solution. Afterwards, the active ingredient and then the other components were dissolved in the B46 dispersion. The obtain mixture was magnetically stirred for 3 h.

The plasters were prepared by using a laboratory-coating unit Mathis LTE-S(M) (Mathis, CH) equipped with a blade coater. The mixture was spread on the release liner at the constant rate of 1 m/min. The coating thickness was fixed at 300 μm in order to obtain a dried matrix with a thickness of about 70 μm. The systems were dried at 50 °C for 20 min, covered with the backing layer, sealed in an airtight container and stored at 25 ± 1 °C.

The final composition of the dried plaster matrices is reported in Table 1.

2.5. Drug content

A plaster sample of 2.54 cm^2 was dissolved in 20 mL of ethyl acetate and diluted in 10 mL of mobile phase (HPLC grade). The solutions were filtered (Durapore® membrane, pore size 0.45 μm; Millex GV, Millipore Corporation, USA) and assayed by the HPLC method reported in Section 2.8. Each value represents the mean of three determinations.

2.6. In vitro release studies

The dissolution test was performed using an apparatus SR8 PLUS Dissolution test station (Hanson Research, CA, USA) according to the Disk Method of the European Pharmacopoeia (Ph. Eur. VI Ed.). A plaster sample of 8.04 cm^2 was placed flat on the disk with the release surface facing up. The back of the plaster was attached on the disk by using a cyanoacrylate adhesive. The experiment was performed by using 500 mL of deionized water as dissolution medium maintained at 32 ± 0.5 °C and stirred at 50 rpm. At fixed intervals, the dissolved amount of IB released from the plasters was spectrophotometrically determined at 227 nm wavelength. The results are expressed as mean of three samples.

The release rate constant was calculated according to Higuchi's equation (Minghetti et al., 1999) as follows:

$$\frac{M_t}{M_\infty} = kt^{-0.5} \quad (1)$$

where M_t is the amount of drug released at time t, M_∞ is the drug loading in the matrix, and k is the release rate constant expressed as h^{-1}.

2.7. Ex vivo human skin permeation studies

The skin used in the transdermal permeation studies was obtained from the abdomen of three different patients who underwent cosmetic surgery. The full-thickness skin was sealed in evacuated plastic bags and frozen at −20 °C within 24 h after removal. Prior to preparation, the skin was de-frozen to room temperature, and the excess fat was carefully removed. The skin sections were cut into squares and, after immersing the skin in water at 60 °C for 1 min, the human epidermis was gently separated from the remaining tissue with forceps. Prior to experimental use, the sample was carefully inspected for any defects before mounting them onto the Franz diffusion cells with the epidermis facing upwards and the stratum corneous side in contact with the sample. In the case of saturated solutions of *S*-IB and *RS*-IB, the upper and lower parts of the Franz cell were sealed with Parafilm® and fastened together by means of a clamp, with the human epidermis specimen acting as a seal between the donor and receptor compartments and, therefore, the donor compartment was filled by 0.5 mL of the saturated solution and closed. In the case of the medicated plasters, a sample of 2.54 cm^2 was applied to the diffusion cell as donor phase before sealing the two compartments. The

Table 1
Composition of the matrices (% w/w), technological characterization and skin permeability data of plasters.

Form. no.	Matrix composition					Technological characterization				Permeability data	
	S-IB	IB	PG	B46	EuRL	Drug content (μg/cm^2)	Crystall. time (days)	Peel adhesion (cN/cm)	Holding power (days)	PA24 (μg/cm^2)	J_{max} (μg/cm^2/h)
1	3.0		–	97.0	–	280 ± 9	28	691 ± 28	>3	318 ± 94	–[a]
2	3.0		4.0	93.0	–	367 ± 23	60	607 ± 48	>3	390 ± 104	15 ± 4
3	3.0		–	94.0	3.0	367 ± 39	60	552 ± 34	>3	271 ± 54	12 ± 2
4	3.0		4.0	90.0	3.0	317 ± 45	>180	422 ± 15	>3	338 ± 56	14 ± 3
5	4.5		4.0	88.5	3.0	–[b]	13	–[b]	–[b]	–[b]	–[b]
6	4.5			91.0	4.5	472 ± 4	60	501 ± 24	>3	427 ± 72	15 ± 2
7	4.5		4.0	87.0	4.5	337 ± 47	>180	435 ± 26	>3	337 ± 47	14 ± 2
8	6.0		–	88.0	6.0	614 ± 4	60	432 ± 45	>3	450 ± 121	18 ± 5
9	6.0		4.0	87.0	3.0	–[b]	4	–[b]	–[b]	–[b]	–[b]
10	6.0		4.0	84.0	6.0	563 ± 25	>180	403 ± 49	>3	370 ± 115	14 ± 4
11		3.0	4.0	90.0	3.0	340 ± 12	–[b]	–[b]	–[b]	292 ± 27	12 ± 2
12		6.0	4.0	84.0	6.0	542 ± 19	–[b]	–[b]	–[b]	–[b]	–[b]

[a] Not calculated.
[b] Not performed.

medicated plasters were stored over a 3-week period before the experiments.

The used vertical cells had a wider column than the original Franz-type diffusion cell, and the bowl shape was removed. They had a diffusion area of 0.636 cm^2 and a 5 mL (approx.) receptor compartment. The receiver volume of each cell was individually calibrated.

The receiver medium constituted of pH 7.4 phosphate buffer saline solution, was continuously stirred with a small magnetic bar and thermostated at 37 ± 1 °C, so that the skin surface temperature was approximately at 32 ± 1 °C. At predetermined times, 0.2 mL samples were withdrawn from the receiver compartment and replaced with fresh receiver medium. Sink conditions were maintained throughout the experiments. Samples were analyzed by HPLC according to the method described in Section 2.8.

2.7.1. Data analysis

The cumulative amount permeated through the skin per unit area was calculated from the concentration of each substance in the receiving medium and plotted as a function of time. The steady flux (J_{max}) was determined as the slope of the linear portion of the plot. The permeability coefficient was calculated according to Fick's first law of diffusion (Eq. (2)):

$$K_p = \frac{J_{max}}{S} \quad (2)$$

where K_p (cm/h) is the permeability coefficient, J_{max} (μg/cm^2 per h) is the flux at the steady state and S is the drug donor concentration (μg/cm^3), corresponding to the drug solubility in the vehicle at 32 °C or the drug content in the plaster used in the permeation experiment.

2.8. Drug assay

The concentration of *S*-IB in the medium was determined by an HPLC assay (HP 1100, Chemstations, Agilent Technologies, USA). A 20 μL sample was injected at 25 °C on a C18 reverse-phase column (C18 Nova-Pak, 4.6 mm × 150 mm, Waters, USA). The wavelength was set at 225 nm. The composition of the eluent was a mixture of acetonitrile and water acidified at pH 2.6 by phosphoric acid (60:40%, v:v) and the flow rate was 1.5 mL/min.

A standard calibration curve (1–50 μg/mL) was used. The limit of quantification was 0.2 μg/mL. Resolution from the background noise was adequate at this level.

2.9. Monitoring crystal formation

Appearance of drug crystals was monitored visually and microscopically (Axioscope, Zeiss, G) throughout an area of 10 cm^2. The monitoring time intervals were daily in the first 2 weeks and then bi-weekly over a 6-month period.

2.10. Adhesion properties evaluation

2.10.1. Peel adhesion 180° test

Two weeks after preparation, a sample of the testing formulation was cut into strips 2.5 cm wide, applied to an adherent plate, smoothed three times with a 4.5 kg roller, maintained for 10 min at 25 °C and pulled from the plate at 180° angle and at the speed rate of 300 mm/min. The 300 mm/min rate and the use of a stainless steel plate were selected as recommended by the standard method PSTC101 (PSTC101). The test was performed with a tensile testing machine Acquati mod. AG/MC 1 (Acquati, I). The force was expressed in cN/cm width of the plaster under test. Peel adhesion values were obtained as averages of three replicates.

2.10.2. Creep resistance test

Two weeks after preparation, the adhesive plasters were cut into strips 2.5 cm wide and 6.0 cm long. Exactly 2.5 cm of the specimen was applied at the tab end of an adherent panel made of stainless steel according to the standard method PSTC107 (PSTC107). The specimen was laid with no pressure exactly parallel to the length of the test surface and smoothed three times with a 4.5 kg roller. The prepared sample was placed in the shear adhesion rack to hold panels 2° inclined from vertical so that the back of each panel formed an angle of 178° with the extended piece of sample. A weight of 500 g was secured to the free end of the plaster. The shear adhesion value is the time required for the sample to separate from the panel. The test was performed with a 8 Bank Oven Shear HT8 instrument (ChemInstrument, USA). Each value is the mean of three replicas.

2.11. Statistical analyses

Treatment of the data involved the use of impair two-tailed Student's *t*-test or One way ANOVA. The α value was set at 0.05 and the null hypothesis assumed the variances between different release profiles to be equal.

3. Results

The stereoisomer exhibited a lower melting point (*S*-IB $T_m = 326.9 \pm 0.1$ K; $\Delta H = 28.32 \pm 0.59$ kJ/mol) than the corresponding racemate (*RS*-IB $T_m = 350.4 \pm 0.0$ K; $\Delta H = 39.45 \pm 1.81$ kJ/mol) and, therefore, a higher solubility (*S*-IB = 127 ± 1 μg/mL; *RS*-IB = 81 ± 1 μg/mL).

3.1. Medicated plaster technological characterization

The data concerning the technological characterization of the plasters are summarized in Table 1. In the plaster containing the lowest amount of *S*-IB, namely 3% w/w in Form. no. 1, drug crystals grew within a 4-week period as well as in the case of the same formulation prepared using *RS*-IB, where the active ingredient crystallized within 25 days (Cilurzo et al., 2005). The induction times of the drug crystallization were also comparable in presence of PG (*RS*-IB crystallization time: 50 days; *S*-IB crystallization time: 60 days) confirming that this excipient acted mainly as a crystallization inhibitor rather than a solubilizing agent (Cilurzo et al., 2005). As verified in the case of the racemate, the addition of both 4% PG and 3% EuRL in Form. no. 4 inhibited the drug nucleation in plaster containing 3% w/w *S*-IB up to 180 days. The inhibition of drug crystallization in the plasters containing the highest percentages of *S*-IB, namely 4.5% w/w and 6% w/w, resulted possible only in presence of PG, keeping constant the *S*-IB/EuRL ratio at 1/1 (Table 1).

As far as the adhesive properties are concerned, all plasters stripped cleanly without leaving any noticeable residue on the plate during the peel adhesion test and the intra-assay standard deviation was always lower than 10%. These features indicated the matrices had good cohesive properties. The addition of EuRL significantly reduced the peel values (Form. nos. 3, 6 and 8 vs Form. no. 1, $p < 0.049$) and the peel adhesion values resulted in agreement to copolymer concentrations found ($R^2 = 0.997$). Furthermore, adding PG to formulation containing EuRL (Form. nos. 4, 7 and 10), the peel adhesion values were significantly demoted ($p < 0.05$, Table 1). The shear adhesion test confirmed the very low creep compliance of the medicated plasters (Table 1). This feature is of particular interest in the case of anti-inflammatory drug loaded plasters which can be applied onto junctures. Indeed, in case of matrices characterized by high creep compliance, a plaster applied onto a junctures could partially detach altering the drug permeation through the skin. Moreover, the plaster can ooze leaving adhesive residues on its outside edges after the application to the skin. Beside of being

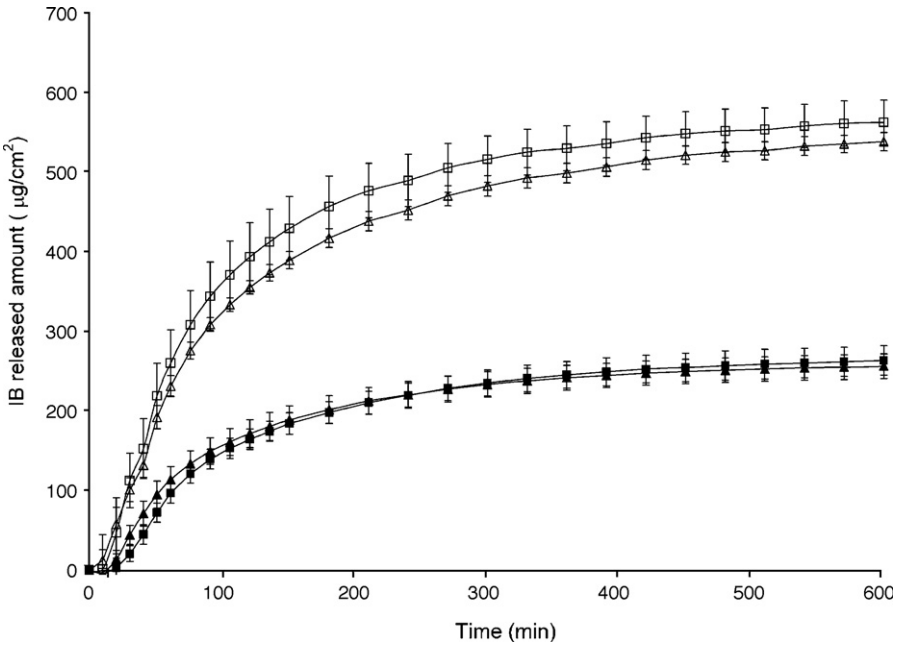

Fig. 1. *In vitro* release profile of *S*-IB from Form. nos. 4 (▲), 10 (△), 11 (■) and 12 (□) (mean ± st. dev., $n = 3$).

un-esthetical, adhesive residues can also collect dirt and stick to cloths or other parts of the body.

As far as the release profiles is concerned, the following remarks can be withdrawn: the amount released from the plasters was dependent on the concentration of the loaded drug (Form. no. 4 vs 10; Form. no. 11 vs 12, Fig. 1), but resulted independent on the use of *S*-IB and *RS*-IB (Form. no. 4 vs 11; Form. no. 10 vs 12, Fig. 1). Even if the amount of drug released from the plaster increased according to the drug content, the release rate constants calculated according to the Higuchi's equation ranged from 0.793 ± 0.032 to $0.825 \pm 0.017\ h^{-1}$ and resulted not statistically different independently on the drug content or the type of the active ingredient used (one way ANOVA, $p = 0.781$).

3.2. Determination of S-IB and RS-IB skin permeation profiles from solutions and plasters

The amount permeated after 24 h (PA24) through the epidermis of the three different donors and the J_{max} of *S*-IB or *RS*-IB from the saturated solutions are summarized in Table 2.

The permeation data of *S*-IB obtained by each donor resulted statistically higher than those of the racemate, either considering all sets of experiments or evaluating the data by the single donor ($p < 0.002$).

The same epidermis donors employed for the saturated solutions were used to determine the skin permeation using Form. nos. 4 and 11 containing 3% w/w *S*-IB and *RS*-IB, respectively. The skin permeability data, reported in Table 2, revealed that no differences were noticeable between the enantiomer and the racemate. Indeed, both the fluxes and the amounts permeated after 24 h of *S*-IB (Form. no. 4) resulted not statistically different with respect to those determined using Form. no. 11 either considering all sets of experiments or evaluating the data by the single donor ($p > 0.17$).

The skin permeation profiles of the medicated plasters containing *S*-IB are summarized in Table 1 and the *S*-IB permeation profiles from Form. nos. 1–4 are shown in Fig. 2 as an example. In the case of the plaster prepared without crystallization inhibitors (Form. no. 1), the permeation profile resulted not linear. Such lack of linearity was attributed to a progressive nucleation process and crystal growth during the experiment and, therefore, to a decrease of the drug activity in the matrix. Indeed, at the end of the permeation experiment, drug crystals were clearly evident in the adhesive matrix by visual inspection.

Furthermore, the drug permeated amounts per square centimetre after 24 h were higher than the drug amount loaded per square centimetre. This pattern is due to the edge effect that led to an overestimation of the cumulative amounts of *S*-IB permeated through skin (Cilurzo et al., 2008; Olivier et al., 2003). This lateral diffusion within the matrix was also clearly relievable in the case of formulation nos. 2–4 containing the 3% w/w of *S*-IB.

The *S*-IB skin permeation profiles, determined using the plasters prepared by adding EuRL, PG or a mixture thereof to the matrix containing 3% w/w *S*-IB (Form. nos. 2–4), resulted superimposable ($p > 0.05$). Increasing the drug and EuRL contents (Form. nos. 3, 6 and 8), the increase of the flux through the human epidermis was found (Table 1). Nevertheless, this trend did not result statistically significant. The presence of PG in Form. nos. 4, 7 and 10 did not further modify the drug permeation profiles (Table 1). The data

Table 2
Permeated amounts after 24 h (PA24) and fluxes (J_{max}) of *RS*-IB or *S*-IB from saturated solutions and two different plaster formulations (mean ± st. dev., $n = 3$).

	S-IB saturated solution		*RS*-IB saturated solution		Form. no. 11		Form. no. 4	
	PA24 (μg/cm²)	J_{max} (μg/cm²/h)	PA24 (μg/cm²)	J_{max} (μg/cm²/h)	PA24 (μg/cm²)	J_{max} (μg/cm²/h)	PA24 (μg/cm²)	J_{max} (μg/cm²/h)
Donor 1	182 ± 19	6 ± 1	307 ± 41	13 ± 2	247 ± 67	10 ± 3	257 ± 36	11 ± 1
Donor 2	109 ± 11	3 ± 0	216 ± 30	9 ± 2	269 ± 62	11 ± 3	234 ± 52	10 ± 2
Donor 3	53 ± 15	2 ± 0	154 ± 2	7 ± 0	186 ± 25	8 ± 1	161 ± 49	7 ± 2
All donors[a]	99 ± 46	4 ± 2	279 ± 121	10 ± 3	234 ± 61	10 ± 2	218 ± 60	8 ± 2

[a] $n = 9$.

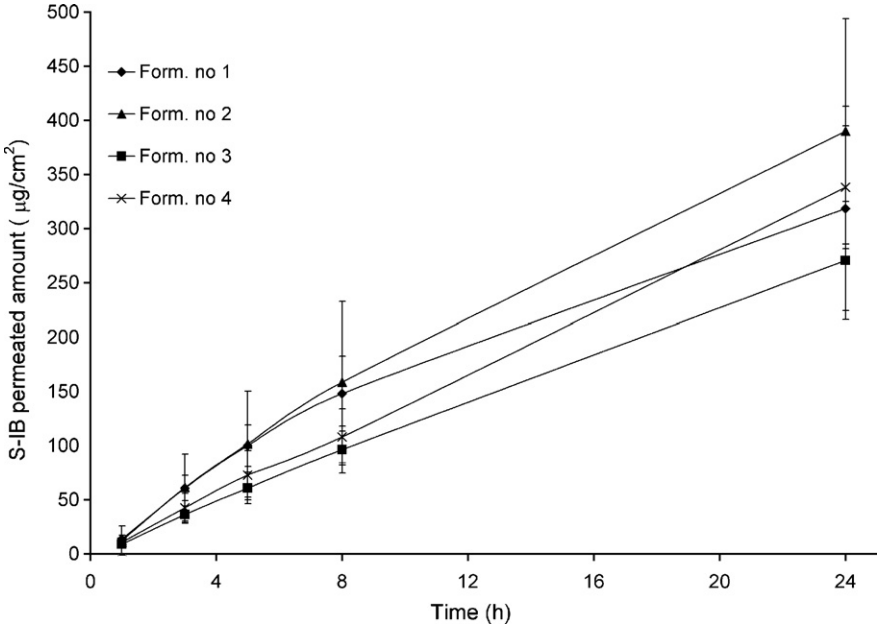

Fig. 2. *S*-IB *ex vivo* skin permeation profile from formulation nos. 1–4 (mean ± st. dev., $n = 3$).

evidenced that the considered formulative variables and the strong increase of the drug content did not improve skin permeation of *S*-IB.

4. Discussion

As far as the *in vitro* human skin permeation studies are concerned, the data obtained from saturated solutions were in agreement with the physico-chemical characteristics of *S*-IB and *RS*-IB. As a matter of fact, it has been reported that enantiomers of chiral compounds with a lower melting point than their racemates, as in the case of *S*-IB and *RS*-IB, have usually higher solubility and, consequently, greater flux through the skin than those of the racemates (Kommuru et al., 1998). The experimental permeation data fit also with the mathematical model, i.e. the melting temperature-membrane transport (MTMT) concept, based on the interdependence of the physico-chemical characteristics, namely melting temperature, and the membrane transport behaviour of a chiral penetrant, which was used to predict the permeability ratio of enantiomers and racemates of chiral molecules (Touitou et al., 1994; Vavrova et al., 2002). According to this model, the ratio of the fluxes of a chiral compound and the corresponding racemate through the skin is mainly dependent upon their solubility and, consequently, a strict relationship between thermal features and skin permeability exists. Such relationship is expressed by the following equation:

$$\ln\frac{J_S}{J_{RS}} = \ln\frac{S_S}{S_{RS}} = \frac{\Delta H_{RS}\cdot(T_{m\,RS}-T)}{R\cdot T_{m\,RS}\cdot T} - \frac{\Delta H_S\cdot(T_{m\,S}-T)}{R\cdot T_{m\,S}\cdot T} \quad (3)$$

where T is temperature at which the experiment is carried out (305 K), R is the universal gas constant and other terms can be interpreted as described in earlier sections.

In our case, the theoretical J_S/J_{RS} value, calculated according to the equation reported above, was 3.55 which resulted very close to the experimental value ($J_{max,S}/J_{max,RS} = 3.00 \pm 0.59$).

If the permeation data obtained by saturated solutions were in agreement with the theory, e.g. the most soluble compound allows to obtain a higher flux, the results obtained by using the plasters were unexpected. Indeed, neither the chirality of ibuprofen nor its concentration in the plaster influenced the permeation process of the drug. Considering that both *RS*-IB and *S*-IB rapidly crystallized in the dried matrix (Table 1), it is reasonable to assume that both the active ingredients were in a supersaturated condition in the plasters (Cilurzo et al., 2005). Even if it was not possible to determine experimentally the solubility of *RS*-IB and *S*-IB in the plaster matrix, on the bases of their thermal data, the solubility of *RS*-IB would be lower with respect to that of *S*-IB. As a consequence, considering that the concentrations of the pure enantiomer and racemate are identical in Form. nos. 4 and 11 (Table 1), the supersaturation degree of *S*-IB should be lower than that of *RS*-IB and, therefore, the *S*-IB flux should result lower than that measured for *RS*-IB. The lack of differences in the $J_{max,S}$ and $J_{max,RS}$ could be justified supposing that the drug thermodynamic activity in the adhesive matrix was not the main limiting step in the permeation process, but other factors could deeply influence the drug release from the plasters. This hypothesis was also supported by testing the plasters loaded at 4.5% w/w and 6% w/w *S*-IB which evidenced no improvements in drug flux through the skin (Table 1). This lack of differences in the *in vitro* release rate constants verified by the dissolution test indicated also that the skin absorption of ibuprofen vehicled in the plasters was probably limited by its diffusivity in the adhesive matrix rather than its diffusion through the human epidermis.

5. Conclusion

The statistical analyses revealed that the J_{max} of *S*-IB vehicled in saturated solution resulted higher than that of *RS*-IB according to the theory. When supersaturated silicon plasters were used, the flux through the skin resulted independent of the drug loading and chirality. The comparison of all sets of permeation data evidenced that depending on the vehicle and the use of racemate or enantiomer, the ibuprofen fluxes followed the rank order: *S*-IB vehicled in the saturated solution > *S*-IB vehicled a in plaster ≅ *RS*-IB vehicled in a plaster > *RS*-IB vehicled in the saturated solution.

In conclusion, the proposed plasters containing *RS*-IB determined a significant increase of the flux with respect to the corresponding saturated solution; when *S*-IB was used, the enhancement effect of the supersaturation was limited by the diffusivity of the active ingredient in the silicon matrix.

References

Cheng, H., Rogers, J.D., Demetriades, J.L., Holland, S.D., Seibold, J.R., Depuy, E., 1994. Pharmacokinetics and bioinversion of ibuprofen enantiomers in humans. Pharm. Res. 11, 824–830.

Cilurzo, F., Minghetti, P., Casiraghi, A., Tosi, L., Pagani, S., Montanari, L., 2005. Polymethacrylates as crystallization inhibitors in monolayer transdermal plasters containing ibuprofen. Eur. J. Pharm. Biopharm. 60, 61–66.

Cilurzo, F., Minghetti, P., Pagani, S., Casiraghi, A., Montanari, L., 2008. Design and characterization of an adhesive matrix based on a poly(ethylacrylate, methyl methacrylate). AAPS PharmSciTech 9, 748–756.

Iervolino, M, Cappello, B., Raghavan, S.L., Hadgraft, J., 2001. Penetration enhancement of ibuprofen from supersaturated solutions through human skin. Int. J. Pharm. 212, 131–141.

Kommuru, T.R., Khan, M.A., Reddy, I.K., 1998. Racemate and enantiomers of ketoprofen: phase diagram, thermodynamic studies skin permeability, and use of chiral permeation enhancers. J. Pharm. Sci. 87, 833–840.

Millership, J.S., Collier, P.S., 1997. Topical administration of racemic ibuprofen. Chirality 9, 313–316.

Minghetti, P., Cilurzo, F., Casiraghi, A., Molla, F.A., Montanari, L., 1999. Dermal patches for the controlled release of miconazole: influence of the drug concentration on the technological characteristics. Drug Dev, Ind. Pharm. 25, 679–684.

Olivier, J.C., Rabouan, S., Couet, W., 2003. In vitro comparative studies of two marketed transdermal nicotine delivery systems: Nicopatch® and Nicorette®. Int. J. Pharm. 252, 133–140.

PSTC-101 International Standard for Peel Adhesion of Pressure Sensitive Tape, revised 6/00, 2000. Test Methods for Pressure Sensitive Adhesive Tapes, 13th edition. Pressure Sensitive Tape Council, Stonebridge Lane, Illinois, pp. 23–30.

PSTC-107 International standard for shear adhesion of pressure sensitive tape, revised 10/00, 2000. Test Methods for Pressure Sensitive Adhesive Tapes, 13th edition. Pressure Sensitive Tape Council, Stonebridge Lane, Illinois, pp. 37–44.

Tegeder, I., Muth-Selbach, U., Lotsch, J., Rusing, G., Oelkers, R., Brune, K., Meller, S., Kelm, G.R., Sorgel, F., Geisslinger, G., 1999. Application of microdialysis for the determination of muscle and subcutaneous tissue concentrations after oral and topical ibuprofen administration. Clin. Pharmacol. Ther. 65, 357–368.

Touitou, E., Chow, D.D., Lawter, J.R., 1994. Chiral β-blockers for transdermal delivery. Int. J. Pharm. 104, 19–28.

Vavrova, K., Hrabalek, A., Dolezal, P., 2002. Enhancement effects of (R) and (S) enantiomers and the racemate of a model enhancer on permeation of theophylline through human skin. Arch. Dermatol. Res. 294, 383–385.